Kinetics of uranium(VI) lability and solubility in aerobic soils

M. Izquierdo[ab]*, S.D. Young[a], E.H. Bailey[a], N.M.J. Crout[a], S. Lofts[c], S.R. Chenery[d] and G. Shaw[a]

[a]School of Biosciences, University of Nottingham, Sutton Bonington Campus, Loughborough, LE12 5RD, United Kingdom
[b]Institute of Environmental Assessment and Water Research, 18-26 Jordi Girona, Barcelona 08034, Spain
[c]UK Centre for Ecology and Hydrology, Lancaster Environment Centre, Library Avenue, Bailrigg, Lancaster, LA1 4AP, United Kingdom
[d]British Geological Survey, Environmental Science Centre, Keyworth, Nottingham, NG12 5GG, United Kingdom
*corresponding author: maria.izquierdo@idaea.csic.es Tel. +34934006146

ABSTRACT

Uranium may pose a hazard to ecosystems and human health due to its chemotoxic and radiotoxic properties. The long half-life of many U isotopes and their ability to migrate raise concerns over disposal of radioactive wastes. This work examines the long-term U bioavailability in aerobic soils following direct deposition or transport to the surface and addresses two questions: (i) to what extent do soil properties control the kinetics of U speciation changes in soils and (ii) over what experimental timescales must U reaction kinetics be measured to reliably predict long-term of impact in the terrestrial environment? Soil microcosms spiked with soluble uranyl were incubated for 1.7 years. Changes in U^{VI} fractionation were periodically monitored by soil extractions and isotopic dilution techniques, shedding light on the binding strength of uranyl onto the solid phase. Uranyl sorption was rapid and strongly buffered by soil Fe oxides, but U^{VI} remained reversibly held and geochemically reactive. The pool of uranyl species able to replenish the soil solution through several equilibrium reactions is substantially larger than might be anticipated from typical chemical extractions and remarkably similar across different soils despite contrasting soil properties. Modelled kinetic parameters indicate that labile U^{VI} declines very slowly, suggesting that the processes and transformations transferring uranyl to an intractable sink progress at a slow rate regardless of soil characteristics. This is of relevance in the context of radioecological assessments, given that soil solution is the key reservoir for plant uptake.

Keywords: uranium, soil, humus, iron oxide, bioavailability, isotopic dilution

1. INTRODUCTION

Uranium is considered a potential hazard to ecosystems and human health due to its chemotoxic and radiotoxic properties (Alloway, 2012). Contamination is widespread (Gavrilescu et al., 2009); sources include nuclear weapons, nuclear reactor operations, nuclear accidents, waste disposal (Vandenhove et al., 2007a) and mining activities (Lottermoser et al., 2011). In reducing environments, tetravalent U^{IV} is typically present as insoluble uraninite $U^{IV}O_2(s)$, although numerous recent works have identified non-crystalline disordered U^{IV} phases in soils and sediments (Fuller et al. 2020 and references therein). Under oxidising conditions, U^{VI} as the uranyl cation ($U^{VI}O_2^{2+}$) is the common species. Uranyl is relatively mobile (Cumberland et al., 2016) and is the major species responsible for U toxicity in aquatic organisms (Crawford et al., 2017). The presence of complexing ligands in groundwater may enhances U mobility. Thus, groundwater interactions with waste deposits influence safety assessment of radioactive waste repositories (Krupka et al., 1999; Um et al., 2010; Vandenhove et al., 2007a). The long half-life of many U isotopes (i.e. $10^5 – 10^8$ yr) and their ability to migrate as complexed and free uranyl forms raise concerns over geological disposal of radioactive wastes.

Radioisotope solubility is often expressed as a solid-liquid distribution coefficient (K_d); compilations exist for U (e.g. Crawford et al. 2017; Krupka et al., 1999; Sheppard et al., 2006, 2009). Values of K_d are typically obtained after 'spiking' soils (Krupka et al., 1999) and incubating these under suitable conditions. However, the resulting data are typically based on relatively short contact times ranging from hours (Manoj et al., 2019) to weeks (Vandenhove et al., 2007a) and, rarely, months (Elless and Lee, 1998). Such an approach is unlikely, therefore, to provide true 'equilibrium' K_d values. The large variation seen in compilations of U K_d values largely reflects a strong dependence on soil properties, especially pH (Sheppard et al., 2009). Echevarria et al. (2001) found a linear relationship between soil pH and U sorption, whilst soil texture and organic matter were not significant. However, Cumberland et al. (2016) and Fuller et al. (2020) demonstrated the relevance of U complexation with humic substances, which can influence U mobility and K_d values. Thus, K_d values are subject to uncertainties that may compromise disposal risk assessments if site-specific factors are not considered.

Numerous studies have attempted chemical fractionation of U using sequential extractions. Typically, the so-called 'exchangeable' and 'carbonate-bound' fractions are recognised as readily available (Rout et al., 2016). In a pot experiment, Vandenhove et al. (2014) found a relationship between U concentration in the exchangeable fraction of soils and in ryegrass. As a complement to chemical extractions, isotopic dilution assays have the potential to add new insights into time-dependent changes in U speciation. The technique consists on adding a known amount of an isotopic tracer to a soil suspension in equilibrium; the resulting change in isotopic ratios gives an indication of the isotopically exchangeable concentration, which provides a more mechanistically based estimate of the reactive pool (Young et al., 2005, 2006). Hamon et al. (2008) and Midwood (2007) provide descriptions of the principles of the technique. To date very little is known about U isotopic exchangeability in aerobic soils as the literature is limited to contaminated sediments (Bond et al., 2007; Kohler et al., 2004; Um et al., 2010). To our knowledge, changes in U isotopic exchangeability in aerobic soils, and the influence of soil properties, have not been addressed.

In this work we examined time-dependent changes in the lability and solubility of U in a wide range of soils, incubated under aerobic conditions for 1.7 yr following contamination. The study monitored changes in U fractionation, specifically the 'soluble', 'chemically exchangeable' and 'isotopically exchangeable' U fractions, thereby providing mechanistic insights into the kinetics of U adsorption and immobilisation in aerobic soils over time. Ultimately our main aim was to address two questions: (i) to what extent do soil properties control the kinetics of U speciation changes in aerobic soils and (ii) over what experimental timescales must U reaction kinetics be measured in order to make reliable long-term predictions of impact in the terrestrial environment?

2. MATERIALS AND METHODS

2.1. Soil sampling and characterisation

Twenty topsoil samples (0–15 cm depth) with contrasting properties were collected from locations in the UK (Table 1) and sieved to <4 mm. A portion was oven dried (105°C) and ground for acid digestion. This

was undertaken in Savillex™ vials with concentrated, *Primar Plus™* HF, HNO_3 and $HClO_4$ using a stepped heating program up to 160°C. Duplicate certified reference soils and sediments NIST SRM 2711a, NIST 1646a and IRMM BCR-167 and reagent blanks were also digested. Elemental recoveries were >80% for the majority of the certified elements.

Soil pH was measured in 0.01 M $CaCl_2$ suspensions (2.5 L kg^{-1}). Organic C contents (OC) were determined using a FLASH EA1121 CNS analyser. Total free oxides (Fe_{FREE}, Al_{FREE} and Mn_{FREE}) were extracted by shaking soil with Na-citrate and Na-dithionite for 24 h in a 20°C water bath (Olsen and Roscoe, 1982). Estimates of amorphous and poorly crystalline oxides (Fe_{AM}, Al_{AM} and Mn_{AM}) were obtained following extraction in ammonium oxalate and oxalic acid, shaken in darkness for 2 h (Schwertmann, 1973). All filtered solutions (<0.2 µm) were acidified to 2% HNO_3 before analysis.

2.2. Soil microcosm incubation and soil extractions

Portions of ~1.7 kg (dry soil basis) of partially air-dried soils were contaminated with 5000 µg $U^{VI}O_2^{2+}$ per kg dry soil, using a Spex CertiPrep uranium standard solution (10000 µg mL^{-1}) in 2.5% HNO_3 diluted 1-in-4. To this end, approximately 3.4 mL of the U spike were slowly added to each soil while the samples were mechanically stirred (c. 60 rpm) with the aid of a food mixer for 4 minutes to ensure uniform contamination. This represented a 2 – 7 fold increase in background U concentrations, which ranged between 700–5000 µg kg^{-1}. The moisture contents were readjusted with ultrapure water during soil mixing. No attempt was made to achieve a pre-determined water content; rather, a friable but moist consistency was sought to aid soil mixing, which required different volumes of water to be added to individual soils. Each contaminated soil was distributed between three 1 L glass bottles (microcosms) with a hole in the lid to allow gas exchange and incubated in darkness at 10°C for 619 days. The microcosms were regularly hand shaken to aid aeration, and soluble Mn and Fe were monitored during periodic soil extractions as indicators of any redox changes. Further details on the experimental setup and microcosm sampling are reported in Izquierdo et al. (2019).

Changes in soluble U (U_{sol}) were determined by sampling each microcosm and equilibrating the equivalent of 4.0 g dry soil with 20 mL 0.01 M KNO_3 for 16 h on an end-over-end shaker. The soil suspensions

were centrifuged (3000rpm, 20 min) and filtered through cellulose nitrate syringe filters (0.22 µm pore size). An aliquot was adjusted to 2% HNO_3 prior to analysis. The remaining solution was used for dissolved organic carbon (DOC) analysis.

Chemically exchangeable (U_{exch}) and isotopically exchangeable (U_E) fractions of U were simultaneously determined in the same solution extracts. At each sampling time, a portion equivalent to 2.0 g dry soil was equilibrated with 20 mL 1 M $Mg(NO_3)_2$ containing the equivalent of 6 µg $^{233}UO_2^{2+}$ and 6 µg $^{236}UO_2^{2+}$ per kg dry soil. This was prepared from the Certified Reference Material IRMM-3636 with certified mass fractions of ^{233}U and ^{236}U of 50.135% and 49.832% respectively. The soil suspensions were shaken for 36 hours, centrifuged (3000rpm, 30 min) and filtered through 0.22 µm cellulose nitrate filters, and the supernatant was adjusted to 2% HNO_3 prior to analysis.

The values reported in this work are the average of 3 replicated microcosms. The coefficients of variation were typically between 2 – 10% for the three different soils extractions, suggesting that the $U^{VI}O_2^{2+}$ addition was evenly distributed during experimental soil mixing prior to incubation.

2.3. Analyses of solutions and calculations

The acid digests and soil extracts were analysed using ICP-MS (iCAP-Q; Thermo Fisher Scientific, Bremen, Germany) and Ir and Rh as internal standards. Dissolved inorganic carbon (DIC) and DOC were determined using a Shimadzu TOC-Vcp analyser.

The isotopic composition of the soil extracts was determined using ICP-MS with Ir as internal standard. Peak dwell times for ^{233}U, ^{236}U and ^{238}U were 0.5 s, with 450 quadrupole sweeps. The $^{233}U/^{236}U$ spike was included every 12 samples to drift-correct for mass discrimination. The isotopically exchangeable U was estimated from Eq. 1 (Tye et al. 2002):

$$U_E\ (\mu g\ g^{-1}) = {}^{238}U_{ss}\left(K_d^* + \frac{V_{ss}}{w_{soil}}\right) \qquad \text{(Eq. 1)}$$

where $^{238}U_{ss}$ is the concentration of ^{238}U in the solution phase of the soil suspension (µg L^{-1}), V_{ss} is the volume of extractant (L), w_{soil} is the soil mass (kg) and K_d* (L kg^{-1}) is distribution coefficient of the enriched isotope, and therefore also the K_d of the isotopically exchangeable soil U (Eq. 2):

$$K_d^* = \frac{^{23x}UI_{adsorbed}}{^{23x}UI_{ss}} \qquad \text{(Eq. 2)}$$

In Eq 2, $^{23x}UI_{adsorbed}$ is calculated from the difference between the intensities (cps) of ^{233}U and ^{236}U in the spike and their intensities in the suspension solution phase; $^{23x}UI_{ss}$ is the measured intensity of ^{233}U or ^{236}U in the solution phase of the soil suspension.

A standard soil-solution partition coefficient for the soil U was calculated (Eq 3):

$$\mathrm{K}_d\ (L\ kg^{-1}) = \frac{C_0 + C_{spike}}{U_{sol}} \qquad \text{(Eq. 3)}$$

Where C_0 denotes the concentration of native U in soils (µg kg^{-1}), C_{spike} is the U concentration added to soils (µg kg^{-1}) and U_{sol} is the U concentration (µg L^{-1}) in the 0.01 M KNO_3 extracts.

In addition, the partitioning (K_d^L, L kg^{-1}) between adsorbed isotopically exchangeable U and the free uranyl ion in solution was also calculated (Eq. 4) (Mossa et al., 2020).

$$K_d^L(L\ kg^{-1}) = \frac{U_E - U_{sol}}{(UO_2^{2+})_{sol}} \qquad \text{(Eq. 4)}$$

Where U_E is the concentration of isotopically exchangeable U in soils (mol kg^{-1}), U_{sol} (mol kg^{-1}) is the U concentration extracted with 0.01 M KNO_3 and (UO_2^{2+}) is the free ion activity (mol L^{-1}) in the solution phase of the KNO_3 extracts speciated using WHAM7.

2.4. Geochemical speciation

The geochemical speciation model WHAM7 (Lofts and Tipping, 2011) was used to estimate the speciation of U^{VI} in the solution phase of soil suspensions equilibrated in 0.01 M KNO_3. The modelling approach assumes that all U is present as uranyl U^{VI} and simulates uranyl binding to dissolved organic matter and Fe oxide colloids in the solution phase (Lofts et al., 2015). Input data included soil pH, temperature (277K) and solution

concentrations of Na, Mg, Al, K, Ca, Fe, Mn and U. Colloidal (dissolved) fulvic acid (FA) was included, assuming that FA consists of 50% DOC and only 65% is active with respect to ion binding (Tye et al., 2004). The carbonate system was simulated from measured DIC. WHAM7 was used with an augmented database (Lofts et al., 2015). Two modelling scenarios were tested: (i) FA as the only colloidal phase present in the system; (ii) colloidal FA and sub-micron colloidal hydrous ferric oxides (HFO). This was addressed by allowing Fe^{III} to precipitate as colloids with active surface chemistry in the simulation, using binding parameters from Lofts et al. (2015).

Fractionation of labile U across the whole soil-solution system was also attempted. The solid binding phases included (i) oxides, for which the two sets of estimates (Fe_{FREE}, Al_{FREE} and Mn_{FREE}; Fe_{AM}, Al_{AM} and Mn_{AM}) were tested in separate simulations; (ii) particulate humic acid (HA) estimated from OC assuming that 50% consists of active humic material (Buekers et al., 2008); (iii) geocolloidal species actively binding U in solution i.e. FA and HFO, as described above. We also assessed the use of WHAM7 to predict U_{sol} concentrations from basic soil characteristics.

2.5. Modelling U kinetics

Time-dependent reductions in both U_{sol} and U_E concentrations were described using single rate exponential models with an 'offset' representing a persistently soluble or labile fraction, respectively (Eq. 5):

$$U_x(t) = A.e^{-tk} + B \qquad \text{(Eq. 5)}$$

where U_x(t) is the concentration of soluble or labile U at any time t after initial contamination of the soils; *A* is the soluble or labile U (µg kg^{-1}) after 4 days incubation subject to depletion; *B* is the U persistently remaining soluble or labile fraction; *k* is the first-order rate coefficient (t^{-1}) representing the rate of depletion of A. The model was fitted to experimental data from each soil using Microsoft Excel® 'Solver'. The rate coefficients in Eq. 5 were used to estimate the times required to deplete by half the U_{sol} or U_E concentration measured after 4 days (Eq. 6):

$$T_{1/2}\,(days) = \frac{ln(2)}{k} \qquad \text{(Eq. 6)}$$

3. RESULTS AND DISCUSSION

3.1. Soil characterisation

The general properties of the studied soils are reported in Table 1. Organic C varied between 1.7 – 38.6% strongly reflecting different land uses. Soil pH ranged between 3.4 – 8.0, with the lowest values reported for a soil overlying pyrite-rich bedrock and the highest values for calcareous soils. The concentrations of free oxides ranged between 1,180 – 22,700 mg kg^{-1}.

3.2. Soluble U (U_{sol})

U_{sol} kinetics

Figures 1 and 2 show that U_{sol} decreased rapidly, from the initial addition of 5000 µg kg^{-1}, to 2 – 160 µg kg^{-1} in the first 4 days of incubation, probably due to surface complexation and cation exchange reactions (Krupka et al., 1999). Langmuir (1978) demonstrated that maximum UO_2^{2+}sorption on minerals occurs a pH 5–8.5; in acidic organic soils there is greater competition with protons and other metallic cations for adsorption sites. The initially large and rapid U_{sol} removal from solution was followed by a slow decline for 6 months and a subsequent stabilisation, or continued slower decline, for the remainder of the experiment. Earlier studies reported dual rate kinetics for uranyl sorption on Fe oxides and silica; the first sorption step has been shown to be complete within minutes (Hsi and Langmuir, 1985; Langmuir, 1978; Tinnacher et al., 2013). Concentrations of U_{sol} remaining at the end of the experiment were consistent across all soils (1–40 µg kg^{-1}) and least for near-neutral soils with lower OC.

The decline in U_{sol} fitted the exponential model (Figures 1 and 2) throughout the incubation, especially over the longer term (Figure S1). The kinetic parameters are plotted in Figure S2 (and Table S1); the depletion half-times ($T_{1/2}$) ranged between 30 and 250 days suggesting slow U_{sol} sorption kinetics, following the initial sorption at 4 days. The slow decline in U_{sol} has been attributed to inter-particle diffusion, re-distribution to lower reactivity surface sites, precipitation or other mass transfer-limited processes (Rihs et al., 2004; Tinnacher et al., 2013). In practical terms, for the soil with the longest $T_{1/2}$ it would take ca. 5 years to drop below 1% of starting value. Thus, our data and model fits suggest that some soils showed continued sorption

of U beyond 619 days which emphasises the need for studies with extended contact times to inform longer-term risk assessment calculations.

The size of the fraction subject to removal (A) and the persistently soluble fraction (B) appeared to be pH controlled (Figure S2). With increasing pH, both A and B fractions initially declined, passed through a minimum around pH 6 and increased again in calcareous soils with pH>7.5. There was a weak negative relationship between $T_{1/2}$ and OC. Organic ligands may enhance uranyl adsorption onto Fe oxides forming ternary U^{VI}-FA surface complexes (Tinnacher et al., 2013).

U_{sol} speciation using WHAM7

The proportion of predicted species remained largely unchanged over time and therefore median values for thirteen time points are reported (Figure S3). At pH<5, solution speciation was dominated by the free uranyl ion (UO_2^{2+}) (30–94%) and uranyl-colloidal FA complexes (4–66%); <20% was predicted to bind to HFO if this was simulated, and other complexes were minor (<2%). If HFO was not allowed to precipitate in the model run, there were slightly greater free ion activities because of the absence of complexation with HFO and Fe_{sol} competition with UO_2^{2+} for complexation with FA ligands. Greater abundance of uranyl-FA complexes was reported for organic soils (>10% OC). There was a very strong negative correlation (R^2=0.92, n=7) between the abundances of free UO_2^{2+} and uranyl-FA complexes for acidic soils, suggesting that the presence of organic ligands may regulate toxicity. Free ion activity peaked for lower organic, acidic soils with OC<10%.

Solution speciation between pH 5–7 was dominated by complexation with geocolloids. In soils with Fe_{sol} > 100 µg L^{-1}, 80–99.8% U_{sol} was bound to HFO, followed by uranyl-FA complexation (up to 15%). The abundance of free UO_2^{2+} dropped to <1% with increasing pH. However, when the simulation inhibited adsorption to colloidal HFO, either because Fe_{sol} was too low to precipitate or because HFO precipitation was excluded from the model options, complexation with FA was clearly dominant (60–99%), followed by up to 25% free UO_2^{2+}, probably reflecting Fe_{sol}-U_{sol} competition for binding to FA. Uranyl-hydroxides (primarily UO_2OH^+, 1–13%), carbonate complexes such as UO_2CO_3 and $UO_2(CO_3)_2^{2-}$ (1–40%) were also predicted in the absence of HFO. Thus, inclusion of binding to HFO colloids substantially affects apparent U_{sol} speciation and

220 resultant risk assessments. This is of particular relevance given that free ions are the most bioavailable forms
221 of metal and are often considered as the best indicator of toxicity (Khan et al., 2011).

222 U_{sol} in calcareous soils was largely present as carbonate complexes (21–99.8%) as also noted by Krupka
223 et al. (1999). Where precipitation of colloidal HFO was simulated, 20–99% U_{sol} was present as alkaline earth-
224 uranyl-carbonate complexes, primarily $Ca_2UO_2(CO_3)_3$, which rose to 96.9–99.8% in the absence of HFO. In all
225 the modelling scenarios, uranyl-carbonate complexes made a small contribution (<2%), whilst other species
226 including free uranyl were absent at this pH (<0.01%) (Figure S3).

227 *Partition coefficients K_d*

228 Values of K_d (Eq. 3) varied widely with ca. 2,000 L kg^{-1} for acidic soils, 3,000-40,000 L kg^{-1} for neutral soils and
229 300-20,000 L kg^{-1} for calcareous soils (Figure S4). These are within the ranges reported in the literature (Krupka
230 et al., 1999; Kumar et al., 2019; Sheppard et al., 2007). Values increased slightly within the first few months
231 reflecting the gradual decrease in U_{sol} described above (Figure 2). This time-dependency showed little
232 dependence on soil properties. The effect of radionuclide-soil/sediment contact time has implications for
233 radiological risk assessments based upon short-term K_d values.

234 Multiple regression analysis for the whole dataset did not show significant relationships between soil
235 properties and the K_d. This is due to the inconsistent trend with pH around a 'critical' pH of 5.5 as noted by
236 Sheppard et al. (2006). Soil pH controls K_d through regulating both adsorption strength and (soluble)
237 complexation processes. The K_d values in the pH range 3–6 increased with pH ($\log_{10}(K_d)=0.20(pH)+2.5$, $R^2=0.48$,
238 Figure S5) reflecting increasing uranyl adsorption onto negatively charged soil surfaces such OC or
239 sesquioxides. Values of K_d peaked around pH 6–7 and subsequently declined. A weak negative relationship
240 between K_d and pH was evident at pH 6–8 ($\log_{10}(K_d)=-0.46(pH)+7.0$, $R^2=0.28$) reflecting the formation of
241 aqueous alkaline earth-uranyl-carbonate complexes (Figure S3). This is in line with previous observations on
242 U solubility (Echevarria et al., 2001; Sheppard et al., 2006).

3.3. *Chemically exchangeable U (U_{exch})*

For soils between pH 3–7, U_{exch} concentrations in the early stages of incubation (4 days) were 10–200 µg kg^{-1} (Figure 1b) i.e. <3% of the initially added uranyl concentration. This suggests that the initial rapid U_{sol} removal is not associated with simple electrostatically bound, outer-sphere complexation of uranyl ions which would be exchangeable with hydrated Mg^{2+} ions. This is consistent with Hsi and Langmuir (1985) who demonstrated that uranyl ions are strongly sorbed onto Fe oxides.

Soil pH was the main control on U_{exch} with a negative relationship for soils between pH 3–7 (R^2=0.52; Figure S6). Slightly greater U_{exch} concentrations were seen in acidic organic soils (30–200 µg kg^{-1}) compared to near-neutral soils with low humus contents (5–50 µg kg^{-1}). By contrast, U_{exch} concentrations up to 3500 µg kg^{-1} were observed for calcareous soils. Our data indicate that a large proportion (up to 57% of U_{total}) remained chemically exchangeable over the first 4 months i.e. electrostatically held as weakly sorbed uranyl-carbonate complexes. This underlines a potential risk to limestone and chalk aquifers given that overlying Rendzina soils would not retain deposited U^{VI}, but rather enhance transport and discharge to the aquifer. Rout et al. (2016) also found that ca. 50% U^{VI} remained chemically exchangeable in calcareous soils after 1 month. Complexation with carbonate ligands inhibits uranyl adsorption onto Fe oxides (Hsi and Langmuir, 1985; Waite et al., 1994) although Bargar et al. (1999) showed that U^{VI}-carbonate complexes can adsorb on oxide minerals.

Median U_{exch} data indicate a slow decline over the course of the experiment following the trend in U_{sol} (Figure 1). This could be associated with redistribution of sorbed uranyl throughout different reactive surface sites (Tinnacher et al., 2013) leading to progressive migration to stronger binding sites inaccessible for chemical exchange.

3.4. *Isotopically exchangeable U (U_E)*

U_E labile concentrations

Uranyl remained largely isotopically exchangeable throughout the experiment (Figures 1 and 3). This demonstrates that the immediate loss of soluble and exchangeable U^{VI} following contamination does not reflect immobilisation processes. After 365 days, the proportion of isotopically exchangeable U_E ranged

between 50 – 80% of U_{total}. After 619 days, 40 – 60% uranyl added was still in dynamic equilibrium with pore water. These data are broadly consistent with Um et al. (2010), who estimated the isotopically exchangeable U at 50–60% of the total U for contaminated sediments underlying radioactive waste tanks. Thus, even though uranyl ions added to soils were rapidly rendered poorly soluble and weakly exchangeable, yet they remain present in reactive forms despite contrasting soil properties. This contrasts with the literature on U fractionation which tends to regard water soluble and chemically exchangeable fractions as the 'potentially available' U species in the environment (Rout et al., 2016).

Predicting U_E solid speciation

WHAM7 simulations after 619 days (Figure S7) suggest that labile U_E was primarily (>95%) adsorbed onto solid Fe oxides. This suggests that U_E is probably bound as inner-sphere complexes with Fe oxides, remaining available for isotopic exchange yet unavailable for 'indifferent' cation exchange. Additionally, for acidic organic soils (OC>10%), 1–5% of U_E was associated with humic substances in soil. Other pools of U_E were predicted to be <2%.

U_E kinetics

Uranium lability (U_E) declined over time (Figure 1c) but the majority of soils did not appear to reach equilibrium (Figure 3). The decreasing trend was very consistent for all soils, despite their contrasting characteristics (pH, OC, Fe_{AM}) and conformed to the exponential model (Figure S1). In contrast to U_{sol}, there were no relationships between the U_E kinetic parameters (A, B and $T_{1/2}$; Table S2) and soil properties, although average $T_{1/2}$ for soils with near-neutral pH were generally lower. The decline in U_E reflects progressively stronger binding or physical occlusion of U, but the persistence of the labile fraction B (ca. 3000 µg kg^{-1}) indicates a limited capacity for uranyl immobilisation with a long half-life for fixation ($T_{1/2}$ = 100–200 days). These observations indicate that the pool of uranyl species able to replenish the soil solution (i) is substantially larger than might be anticipated from basic chemical extractions; and (ii) declines very slowly suggesting that immobilisation processes progress at a slow rate regardless of soil characteristics. This is of particular relevance in the context of radioecological assessments, given that soil solution is the key reservoir for plant uptake.

293 The progressive immobilisation of uranyl may be caused by desorption and re-adsorption processes.
294 According to the work of Waite et al. (1994) on two-site surface complexation models to predict U^{VI} binding,
295 a small population of high-affinity sites exists on the surface of Fe oxides, randomly distributed among a larger
296 population of relatively low-affinity sites. Thus, uranyl ions may progressively relocate to high-affinity sites
297 with lower rates of isotopic exchange. Krupka et al. (1999) suggested that U^{VI} bound to Fe and Mn oxide phases
298 may not be in isotopic equilibrium with soluble U.

299 Organic matter has also been identified as a potential sink for U^{VI}, although the underlying mechanisms
300 are still unclear (Krupka et al., 1999) as is the involvement of abiotic or biotic reduction processes (Cumberland
301 et al., 2016). Microbial reduction of U^{VI} leading to formation of immobile U^{IV} forms has been extensively
302 documented (Newsome et al., 2014). However, we observed consistent Fe_{sol} and Mn_{sol} concentrations over
303 the course of the experiment (Izquierdo et al. 2019), which suggests that the electrochemical status of the 20
304 soils remained largely unchanged. Thus, any reductive processes leading to formation of U^{IV} may be limited to
305 microenvironments following local exhaustion of O_2 within soil pore microsites, and it may not have
306 progressed much further down the redox ladder, whilst the bulk of the soil remained aerated. In addition,
307 microbially-mediated U^{VI} reduction to U^{IV} and subsequent fixation would be enhanced by decomposable
308 organic matter that can fuel bacterial activity. However, there was no clear evidence for kinetically enhanced
309 fixation rates in organic soils (Figure 3a). Our findings suggest that bioreduction processes play a marginal role
310 in the kinetics of labile U^{VI}. Studies on organic soils naturally enriched in U by Fuller et al. (2020) and
311 Regenspurg et al. (2010) have demonstrated that U was largely complexed with soil organic matter as U^{VI}
312 despite reducing conditions; binding to organic matter appeared to prevent U^{VI} bioreduction. Similarly, Burgos
313 et al. (2007) suggested that complexation of U^{VI} with humic substances may interrupt electron transport to U^{VI}
314 thereby decreasing the potential for reduction. Thus, it is more likely that U_E removal in high organic soils
315 reflects abiotic fixation pathways in which rapid, initial adsorption is followed by re-organisation to more
316 stable complexes (Krupka et al., 1999; Regenspurg et al., 2010).

Although carbonate ligands inhibit U adsorption, the trends in U_E (Figure 3c) also suggest transfer to non-labile forms in calcareous soils, as reported by Cumberland et al. (2016) and Elless and Lee (1998). Synchrotron-based studies by Elzinga et al. (2004) and Rihs et al. (2004) showed surface complexation of uranyl-carbonate species via inner-sphere bonding of U^{VI} with a surface carbonate group, primarily in monodentate coordination. Following U^{VI} adsorption, calcite dissolution and re-precipitation may then result in the slow incorporation of U^{VI} into $CaCO_3$ in non-labile forms.

Partitioning between labile adsorbed U^{VI} and free UO_2^{2+} ions in solution: K_d^L

Solid-liquid partition coefficients (K_d^L) based on isotopically exchangeable U^{VI} and free uranyl in solution provide a more mechanistically rigorous expression of the partitioning of geochemically reactive U^{VI} than conventional K_d expressions. Free uranyl ions are the form most readily accumulated by plant roots (Mitchell et al., 2013) and probably the best indicator of potential toxicity, although U^{VI}-carbonate complexes may also be bioavailable (Vandenhove et al., 2007b). Values of the labile K_d^L are substantially greater than standard solid-to-liquid K_d (Figure S4). Values of $\log_{10}K_d^L$ ranged from 6 – 14 primarily reflecting the strong effect of soil pH (R^2=0.93; Figure 4) on binding of UO_2^{2+} ions to geocolloids. Values of the conventional K_d showed little variation with pH as the stronger binding at high pH was effectively offset by the formation of soluble U-carbonate complexes.

Predicting U_{sol} from U_E

Prediction of U_{sol} concentrations from soil properties and labile U_E using WHAM7 was attempted. Goodness of fit was assessed by calculating Residual Standard Deviation (RSD). Using Fe_{FREE} and Mn_{FREE} as potential adsorption surfaces, together with HA, underestimated U_{sol} (RSD=1.20), probably due to overestimating the surface area available for uranyl binding. Improved predictions were obtained when (i) HA, Fe_{AM} and Mn_{AM} estimates were used as particulate active binding phases and (ii) formation of colloidal HFO with chemically active surface was allowed (RSD=0.74, Figure S7); the majority of U_{sol} data fell along the 1:1 line and within ±1RSD.

Omitting colloidal HFO in the modelling options resulted in poor prediction of U_{sol} (RSD=2.24, Figure S8). There was a systematic bias in the predictions, which widened in near-neutral soils where U_{sol} was low and primarily driven by complexation with HFO/FA colloids. Predictions of U_{sol} were more accurate when complexation reactions with colloidal FA or HFO ligands were marginal: (i) in acidic soils in which aqueous U^{VI} is essentially as free (UO_2^{2+}); and (ii) in calcareous soils, dominated by complexation with carbonate ligands. This emphasises the relevance of colloidal complexes in controlling U^{VI} solubility, particularly within pH 4 – 7.

4. CONCLUSIONS

Following contamination, U^{VI} was rapidly removed from solution and was bound to oxides in soil. This was followed by a slower decline in soluble uranyl following an offset exponential kinetic model. Our data suggest that short-term experiments may not be used reliably to predict long-term solubility and K_d values, which has practical significance in risk assessment calculations for facilities such as radioactive waste repositories.

Uranium remained more soluble in calcareous soils due to complexation with carbonate ligands; data and model predictions suggest that a large proportion of U^{VI} in calcareous soils is electrostatically held as weakly sorbed uranyl-carbonate complexes. These weakly bonded fractions are particularly relevant in some environments; Rendzina soils in calcareous terrains would be inefficient at retaining deposited U^{VI} and would not prevent, but rather enhance, transport, dispersion and discharge to the underlying aquifer.

The comparison between solubility and chemical exchangeability data with isotopic exchangeability provided evidence of the binding strength of uranyl onto soils. Despite the low solubility and exchangeability, the added uranyl was almost fully labile after 4 days. Thus, whilst uranyl sorption is rapid and strongly buffered by Fe oxides present in soil, U^{VI} is still reversibly held and geochemically reactive. The kinetics of labile U is remarkably similar between soils and the time trends are small. For the majority of soils, added U was still undergoing net sorption after 600 days and that ca. 50% uranyl added was still in dynamic equilibrium with pore water after this contact time. Modelled kinetic parameters suggest a timeframe of typically 100–200 days to reduce the initially labile U_E by half. Crucially, these findings indicate that the pool of uranyl species able to

365 replenish the soil solution through dissolution, precipitation, de-sorption or dissociation equilibrium reactions
366 (i) is substantially larger than might be anticipated from chemical extractions typically used in soil science, (ii)
367 declines very slowly suggesting that the processes and transformations conducive to uranyl transfer to an
368 intractable sink progress at a slow rate regardless of soil characteristics. This is of particular relevance in the
369 context of radioecological assessments, given that soil solution is the key reservoir for plant uptake.

370 ACKNOWLEDGMENTS

371 This work was carried out within the TREE (Transfer-Exposure-Effects) consortium within the Radioactivity and
372 the Environment (RATE) programme, funded jointly by the Natural Environment Research Council, Radioactive
373 Waste Management Ltd. and the Environment Agency (grant no. NE/L000504/1). We thank the numerous
374 individuals and agencies who gave permission to sample soils.

375 REFERENCES

376 Alloway, B.J. (2012) Heavy metals in soils: trace metals and metalloids in soils and their bioavailability. Springer
377 Science & Business Media.

378 Bargar, J.R., Reitmeyer, R. and Davis, J.A. (1999) Spectroscopic Confirmation of Uranium(VI)−Carbonato
379 Adsorption Complexes on Hematite. Environ. Sci. Technol. 33, 2481-2484.

380 Bond, D.L., Davis, J.A. and Zachara, J.M. (2007) Uranium (VI) release from contaminated vadose zone
381 sediments: Estimation of potential contributions from dissolution and desorption. Developments in Earth
382 and Environmental Sciences 7, 375-416.

383 Buekers, J., Degryse, F., Maes, A. and Smolders, E. (2008) Modelling the effects of ageing on Cd, Zn, Ni and Cu
384 solubility in soils using an assemblage model. Eur. J. Soil Sci. 59, 1160-1170.

385 Burgos, W.D.S.J.M.D., B.A.; E.E. Roden, J.J. Stone, K.M. Kemner, S.D. Kelly (2007) Soil humic acid decreases
386 biological uranium(vi) reduction by *Shewanella putrefaciens* CN32. Environ. Eng. Sci. 24, 755-761.

387 Crawford, S.E., Lofts, S. and Liber, K. (2017) The role of sediment properties and solution pH in the adsorption
388 of uranium(VI) to freshwater sediments. Environ. Pollut. 220, 873-881.

389 Cumberland, S.A., Douglas, G., Grice, K. and Moreau, J.W. (2016) Uranium mobility in organic matter-rich
390 sediments: A review of geological and geochemical processes. Earth-Sci. Rev. 159, 160-185.

391 Echevarria, G., Sheppard, M.I. and Morel, J. (2001) Effect of pH on the sorption of uranium in soils. J. Environ.
392 Radioactiv. 53, 257-264.

393 Elless, M.P. and Lee, S.Y. (1998) Uranium Solubility of Carbonate-Rich Uranium-Contaminated Soils. Water,
394 Air, Soil Pollut. 107, 147-162.

395 Elzinga, E.J., Tait, C.D., Reeder, R.J., Rector, K.D., Donohoe, R.J. and Morris, D.E. (2004) Spectroscopic
396 investigation of U(VI) sorption at the calcite-water interface. Geochim. Cosmochim. Acta 68, 2437-2448.

Fuller, A.J., Leary, P., Gray, N.D., Davies, H.S., Mosselmans, J.F.W., Cox, F., Robinson, C.H., Pittman, J.K., McCann, C.M., Muir, M., Graham, M.C., Utsunomiya, S., Bower, W.R., Morris, K., Shaw, S., Bots, P., Livens, F.R. and Law, G.T.W. (2020) Organic complexation of U(VI) in reducing soils at a natural analogue site: Implications for uranium transport. Chemosphere 254, 126859.

Gavrilescu, M., Pavel, L.V. and Cretescu, I. (2009) Characterization and remediation of soils contaminated with uranium. J. Hazard. Mater. 163, 475-510.

Hamon, R.E., Parker, D.R. and Lombi, E. (2008) Chapter 6 Advances in Isotopic Dilution Techniques in Trace Element Research: A Review of Methodologies, Benefits, and Limitations, in: Donald, L.S. (Ed.), Advances in Agronomy. Academic Press, pp. 289-343.

Hsi, C.-k.D. and Langmuir, D. (1985) Adsorption of uranyl onto ferric oxyhydroxides: Application of the surface complexation site-binding model. Geochim. Cosmochim. Acta 49, 1931-1941.

Izquierdo, M., Bailey, E.H., Crout, N.M.J., Sanders, H.K., Young, S.D. and Shaw, G.G. (2019) Kinetics of 99Tc speciation in aerobic soils. J. Hazard. Mater., 121762.

Khan, M.S., Zaidi, A., Goel, R. and Musarrat, J. (2011) Biomanagement of metal-contaminated soils. Springer Science & Business Media.

Kohler, M., Curtis, G.P., Meece, D.E. and Davis, J.A. (2004) Methods for Estimating Adsorbed Uranium(VI) and Distribution Coefficients of Contaminated Sediments. Environ. Sci. Technol. 38, 240-247.

Krupka, K.M., Kaplan, D., Whelan, G., Serne, R. and Mattigod, S. (1999) Understanding variation in partition coefficient, Kd, values, in: 402-R-99-004B, E. (Ed.), Volume II: Review of Geochemistry and Available Kd Values, for Cadmium, Cesium, Chromium, Lead, Plutonium, Radon, Strontium, Thorium, Tritium (3H), and Uranium. EPA. United States Environmental Protection Agency.

Kumar, A., Rout, S., Pulhani, V. and Kumar, A.V. (2019) A review on distribution coefficient (Kd) of some selected radionuclides in soil/sediment over the last three decades. J. Radioanal. Nucl. Chem.

Langmuir, D. (1978) Uranium solution-mineral equilibria at low temperatures with applications to sedimentary ore deposits. Geochim. Cosmochim. Acta 42, 547-569.

Lofts, S., Tipping, E. (2011). Assessing WHAM/Model VII against field measurements of free metal ion concentrations: Model performance and the role of uncertainty in parameters and inputs. Environ. Chem. 8, 501-516.

Lofts, S., Fevrier, L., Horemans, N., Gilbin, R., Bruggeman, C. and Vandenhove, H. (2015) Assessment of co-contaminant effects on uranium and thorium speciation in freshwater using geochemical modelling. J. Environ. Radioactiv. 149, 99-109.

Lottermoser, B.G., Schnug, E. and Haneklaus, S. (2011) Cola soft drinks for evaluating the bioaccessibility of uranium in contaminated mine soils. Sci. Total Environ. 409, 3512-3519.

Manoj, S., Thirumurugan, M. and Elango, L. (2019) Determination of distribution coefficient of uranium from physical and chemical properties of soil. Chemosphere, 125411.

Midwood, A.J. (2007) Stable Isotope Methods for Estimating the Labile Metal Content of Soils, in: Willey, N. (Ed.), Phytoremediation. Methods and Reviews Humana Press, pp. 149-159.

Mitchell, N., Pérez-Sánchez, D. and Thorne, M.C. (2013) A review of the behaviour of U-238 series radionuclides in soils and plants. J. Radiol. Prot. 33, R17-R48.

Mossa, A.-W., Bailey, E.H., Usman, A., Young, S.D. and Crout, N.M.J. (2020) The impact of long-term biosolids application (>100 years) on soil metal dynamics. Sci. Total Environ., 137441.

Newsome, L., Morris, K. and Lloyd, J.R. (2014) The biogeochemistry and bioremediation of uranium and other priority radionuclides. Chem. Geol. 363, 164-184.

Olsen, R. V., Roscoe E.J.R., Methods of Soil Analysis: Part 2—Chemical and Microbiological Properties, ed. A. L. Page, R. H. Miller and D. R. Keeney, Madison, WI, 1982, pp. 301–312

Regenspurg, S., Margot-Roquier, C., Harfouche, M., Froidevaux, P., Steinmann, P., Junier, P. and Bernier-Latmani, R. (2010) Speciation of naturally-accumulated uranium in an organic-rich soil of an alpine region (Switzerland). Geochim. Cosmochim. Acta 74, 2082-2098.

Rihs, S., Sturchio, N.C., Orlandini, K., Cheng, L., Teng, H., Fenter, P. and Bedzyk, M.J. (2004) Interaction of Uranyl with Calcite in the Presence of EDTA. Environ. Sci. Technol. 38, 5078-5086.

Rout, S., Kumar, A., Ravi, P.M. and Tripathi, R.M. (2016) Understanding the solid phase chemical fractionation of uranium in soil and effect of ageing. J. Hazard. Mater. 317, 457-465.

Schwertmann, U. (1973) Use of oxalate for Fe extraction from soils. Can. J. Soil Sci. 53, 244-246.

Sheppard, M.I., Sheppard, S.C. and Grant, C.A. (2007) Solid/liquid partition coefficients to model trace element critical loads for agricultural soils in Canada. Can. J. Soil Sci. 87, 189-201.

Sheppard, S., Long, J., Sanipelli, B. and Sohlenius, G. (2009) Solid/liquid partition coefficients (Kd) for selected soils and sediments at Forsmark and Laxemar-Simpevarp, in: 1402-3091, I., R-09-27, S.R. (Eds.). Swedish Nuclear Fuel and Waste Management Co.

Sheppard, S.C., Sheppard, M.I., Tait, J.C. and Sanipelli, B.L. (2006) Revision and meta-analysis of selected biosphere parameter values for chlorine, iodine, neptunium, radium, radon and uranium. J. Environ. Radioactiv. 89, 115-137.

Tinnacher, R.M., Nico, P.S., Davis, J.A. and Honeyman, B.D. (2013) Effects of Fulvic Acid on Uranium(VI) Sorption Kinetics. Environ. Sci. Technol. 47, 6214-6222.

Tye, A.M., Young, S., Crout, N.M.J., Zhang, H., Preston, Bailey, E., Davison, W., McGrath, S.P., Paton G. I. and Kilham, K. (2002) Predicting arsenic solubility in contaminated soils using isotopic dilution techniques. Environ. Sci. Technol. 36, 982–988.

Tye, A.M., Young, S., Crout, N.M.J., Zhang, H., Preston, S., Zhao, F.J. and McGrath, S.P. (2004) Speciation and solubility of Cu, Ni and Pb in contaminated soils. Eur. J. Soil Sci. 55, 579-590.

Um, W., Icenhower, J.P., Brown, C.F., Serne, R.J., Wang, Z., Dodge, C.J. and Francis, A.J. (2010) Characterization of uranium-contaminated sediments from beneath a nuclear waste storage tank from Hanford, Washington: Implications for contaminant transport and fate. Geochim. Cosmochim. Acta 74, 1363-1380.

Vandenhove, H., Van Hees, M., Wouters, K. and Wannijn, J. (2007a). Can we predict uranium bioavailability based on soil parameters? Part 1: Effect of soil parameters on soil solution uranium concentration. Environ. Pollut. 145, 587-595.

Vandenhove, H., Van Hees, M., Wannijn, J., Wouters, K. and Wang, L. (2007b) Can we predict uranium bioavailability based on soil parameters? Part 2: soil solution uranium concentration is not a good bioavailability index. Environ. Pollut. 145, 577-586.

Vandenhove, H., Vanhoudt, N., Duquène, L., Antunes, K. and Wannijn, J. (2014) Comparison of two sequential extraction procedures for uranium fractionation in contaminated soils. J. Environ. Radioactiv. 137, 1-9.

Waite, T., Davis, J., Payne, T., Waychunas, G. and Xu, N. (1994) Uranium (VI) adsorption to ferrihydrite: Application of a surface complexation model. Geochim. Cosmochim. Acta 58, 5465-5478.

Young, S.D., Zhang, H., Tye, A.M., Maxted, A., Thums, C. and Thornton, I. (2005) Characterizing the availability of metals in contaminated soils. I. The solid phase: sequential extraction and isotopic dilution. Soil Use Manage. 21, 450-458.

481 Young, S.D., Crout, N., Hutchinson, J., Tye, A., Tandy, S. and Nakhone, L. (2006) Techniques for measuring
482 attenuation: isotopic dilution methods in: R. Hamon, M.M., E. Lombi (Ed.), Natural Attenuation of Trace
483 Element Availability in Soils CRC Press, Boca Raton, FL, pp. 19-55.

Table 1. Location and general properties of the soils in this study, listed in order of land use. Bdl denotes below the detection limit.

				%	%		total concentrations mg kg^{-1}				Free amorphous oxides mg kg^{-1}			Total free oxides mg kg^{-1}			incubation moisture content
code	land use	Latitude	Longitude	inorg C	organic C	pH	U (native)	Al	Mn	Fe	Al	Mn	Fe	Al	Mn	Fe	% wt
CO-A	arable	52° 49' 36.9" N	1° 13' 35.08" W	Bdl	2.3	6.37	1799	26707	508	20965	633	317	3386	751	356	9372	9
EV-A	arable	52° 50' 39.43" N	1° 11' 25.83" W	0.043	2.6	6.04	2336	43275	934	34961	1244	622	4233	1245	736	14217	12
NP-A	arable	52° 51' 38.39" N	1° 7' 30.47" W	Bdl	1.7	6.76	1269	15873	501	17725	637	277	2103	617	331	7531	9
SR-A	arable	52° 51' 3.19" N	0°40'35.01"W	5.33	3.8	7.77	1464	23207	682	22515	1333	232	1181	1176	364	12425	9
WK-A	arable	52° 49' 47.96" N	1° 14' 24.12" W	Bdl	2.4	5.31	1458	19815	645	29614	762	404	3688	842	414	9270	13
WS-A	arable	52° 51' 9.31" N	1° 7' 36.4" W	0.74	2.6	7.71	2181	42149	1037	33255	604	349	1205	456	431	7166	14
BH-G	grassland	52° 48'24.77"N	1°23'58.86"W	1.16	6.2	7.36	4926	27237	4451	30438	1487	3143	5184	1110	3525	14599	20
DY-G	grassland	53° 18'55.30"N	1° 36'1.37"W	Bdl	11.4	3.90	722	15841	43	6925	863	18	2264	1089	36	5563	31
FD-G	grassland	52° 49' 54.13" N	1° 13' 35.92" W	Bdl	5.7	6.19	3177	57058	1053	52789	1626	505	8148	1130	679	18387	24
SB-G	grassland	52° 47' 23.53" N	1° 27' 58.07" W	Bdl	5.0	6.02	1710	22103	460	13775	1181	289	5436	1294	331	10073	15
SR-G	grassland	52° 51' 0.83" N	0° 40' 39.93"W	0.38	5.7	7.04	1651	36862	874	50808	1985	529	3893	1956	666	22668	22
TK-G	grassland	52° 47' 36.62" N	1° 28' 29.94" W	Bdl	6.3	5.32	2825	40942	303	25256	2041	160	7069	1904	165	11484	20
BC-M	moorland	53° 12'44.29"N	1° 5'33.07"W	bdl	5.5	4.18	1477	21124	77	16124	876	6	4841	995	22	7850	15
DY-M	moorland	53° 18'42.34"N	1° 35'59.93"W	Bdl	38.6	3.46	1037	10439	43	5759	2430	18	3421	2987	24	3940	36
BH-W	woodland	52° 48'23.80"N	1°24'5.18"W	2.83	7.5	7.47	2245	23500	2724	25395	880	1398	3126	675	1535	10514	16
BY-W	woodland	52° 49' 42.66" N	1° 27' 51.02" W	Bdl	10.6	3.41	2461	30226	141	22966	1347	55	6978	1634	90	14285	21
IH-W	woodland	52° 44' 54.74" N	1° 17' 51.89" W	Bdl	9.5	3.88	1905	27554	185	18013	1604	60	4178	1826	95	9496	20
PE-W	woodland	53° 12'44.41"N	1° 5'53.23"W	Bdl	7.1	3.82	1076	18022	91	7655	670	38	1806	756	55	4720	12
SR-W	woodland	52° 50' 58.28" N	0°40' 33.61"W	3.75	5.2	8.00	1180	28029	694	25431	1813	321	1650	-	-	-	13
WK-W	woodland	52° 49' 51.48" N	1° 14' 17.8" W	Bdl	24.4	3.87	838	11025	233	13202	1365	143	3578	1444	198	5778	37

FIGURE CAPTIONS

Figure 1. Changes in the concentrations of U in the soluble (a), chemically exchangeable (b), and labile or isotopically exchangeable pools (c) over the course of 619 days incubation in 20 soils. Circles and whiskers denote median values and interquartile (25–75%) range for all soils within the specified pH interval categories, respectively. For U_{sol} and U_E median values, single exponential models have been fitted. The red arrow denotes the concentration of natural U added to soils.

Figure 2. Kinetics of removal of U_{sol} from the soluble (0.01 M KNO_3 extractable) pool in acidic (pH<5) (a), near-neutral (pH 5–7) (b) and calcareous (pH<7) (c) soils over the course of 619 days. The points are experimental data through which an offset single exponential model has been fitted. Soil codes are listed in Table 1.

Figure 3. Kinetics of the isotopically exchangeable (labile) U_E in acidic (pH<5) (a), near-neutral (pH 5–7) (b) and calcareous (pH<7) (c) soils over the course of 619 days. The points are experimental data through which an offset single exponential model has been fitted. Soil codes are listed in Table 1.

Figure 4. Relationship between soil pH and the labile log K_d^L after 619 days incubation.

Figure 1

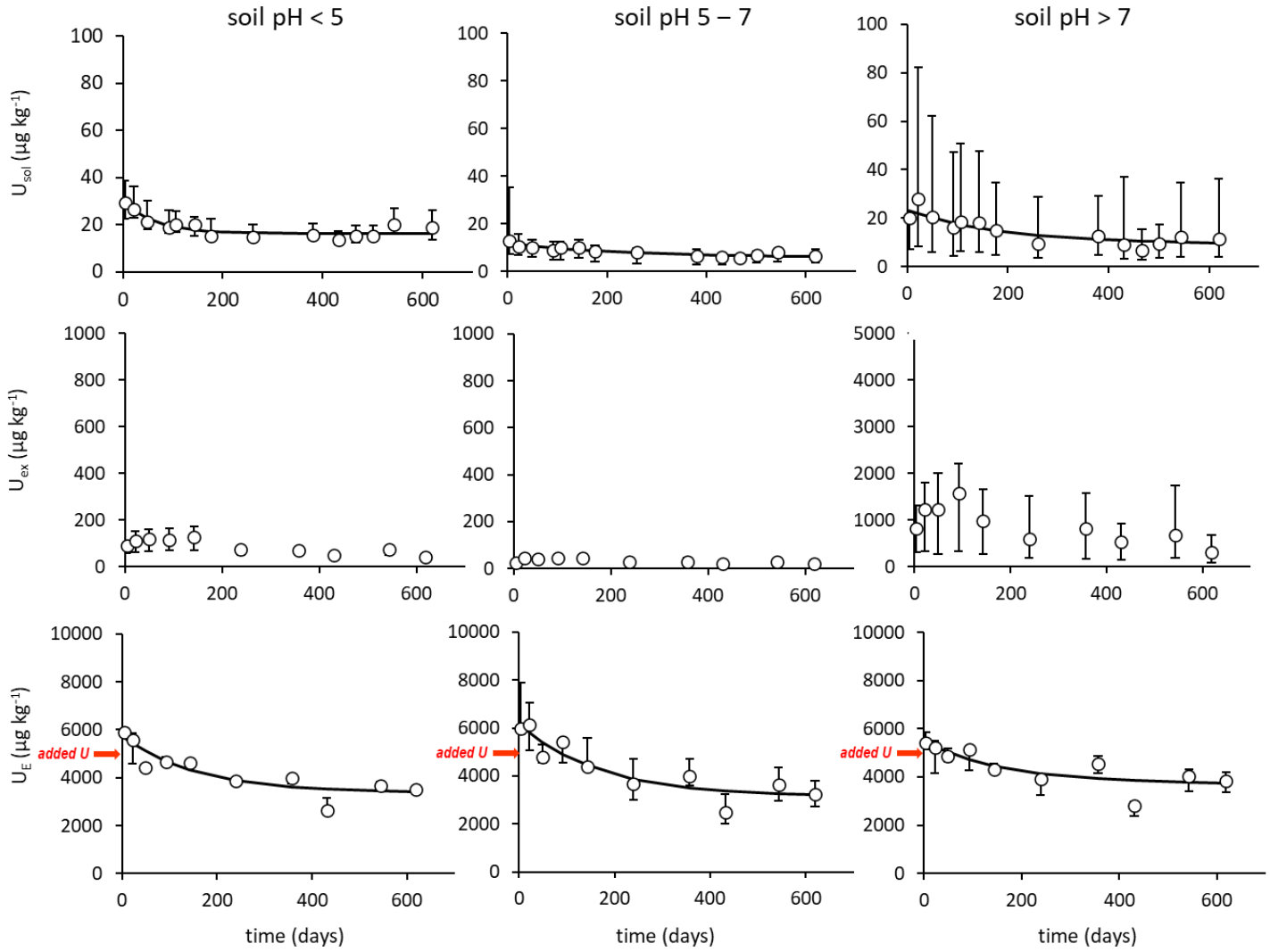
soil pH < 5
soil pH 5 – 7
soil pH > 7
U_{sol} (µg kg^{-1})
U_{ex} (µg kg^{-1})
U_E (µg kg^{-1})
added U
time (days)

Figure 2

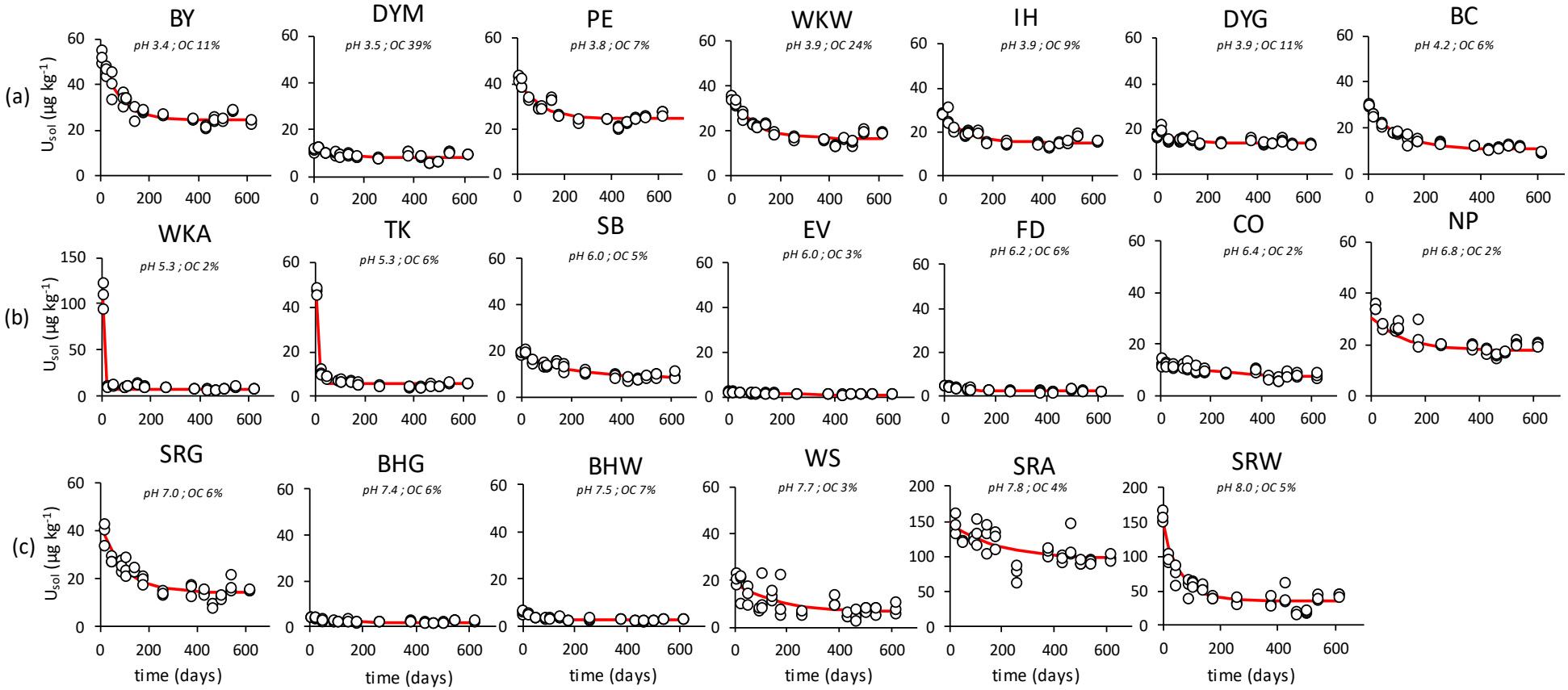
(a)
(b)
(c)
BY
pH 3.4 ; OC 11%
DYM
pH 3.5 ; OC 39%
PE
pH 3.8 ; OC 7%
WKW
pH 3.9 ; OC 24%
IH
pH 3.9 ; OC 9%
DYG
pH 3.9 ; OC 11%
BC
pH 4.2 ; OC 6%
WKA
pH 5.3 ; OC 2%
TK
pH 5.3 ; OC 6%
SB
pH 6.0 ; OC 5%
EV
pH 6.0 ; OC 3%
FD
pH 6.2 ; OC 6%
CO
pH 6.4 ; OC 2%
NP
pH 6.8 ; OC 2%
SRG
pH 7.0 ; OC 6%
BHG
pH 7.4 ; OC 6%
BHW
pH 7.5 ; OC 7%
WS
pH 7.7 ; OC 3%
SRA
pH 7.8 ; OC 4%
SRW
pH 8.0 ; OC 5%
U_sol (µg kg-1)
time (days)

Figure 3

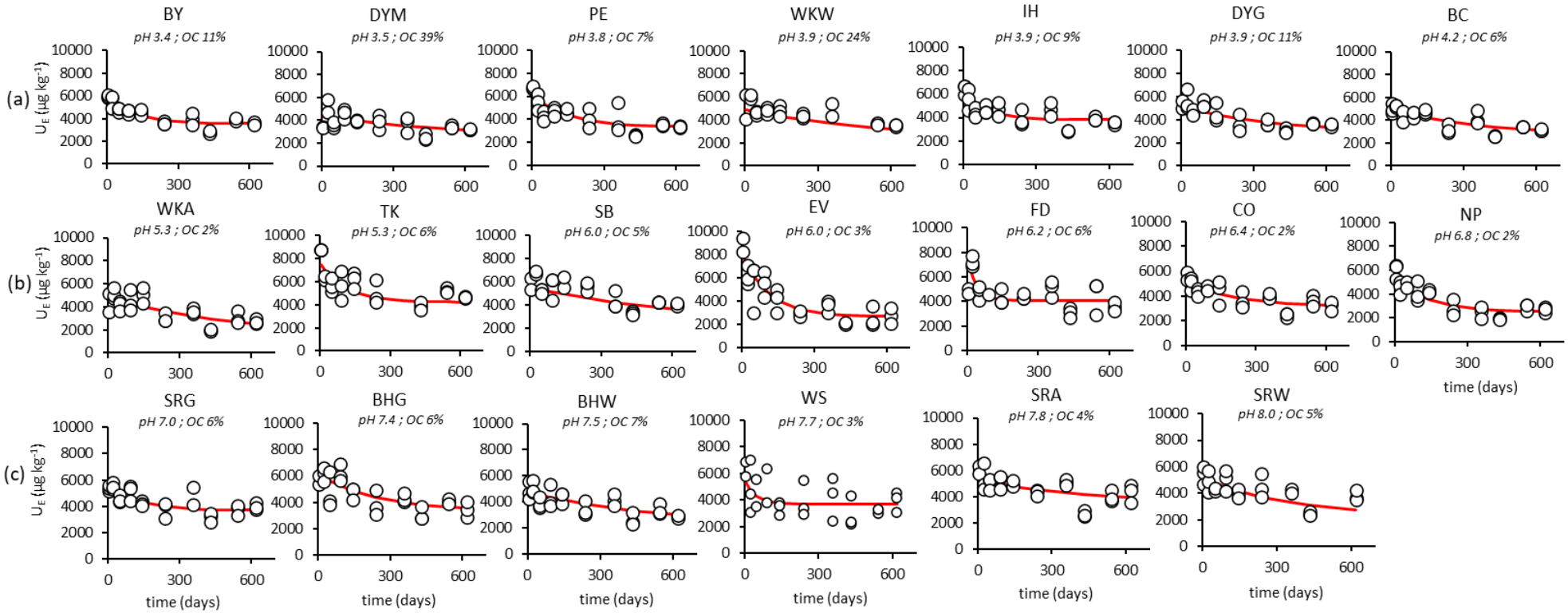
(a)
(b)
(c)
U_E (µg kg^{-1})
BY
pH 3.4 ; OC 11%
DYM
pH 3.5 ; OC 39%
PE
pH 3.8 ; OC 7%
WKW
pH 3.9 ; OC 24%
IH
pH 3.9 ; OC 9%
DYG
pH 3.9 ; OC 11%
BC
pH 4.2 ; OC 6%
WKA
pH 5.3 ; OC 2%
TK
pH 5.3 ; OC 6%
SB
pH 6.0 ; OC 5%
EV
pH 6.0 ; OC 3%
FD
pH 6.2 ; OC 6%
CO
pH 6.4 ; OC 2%
NP
pH 6.8 ; OC 2%
SRG
pH 7.0 ; OC 6%
BHG
pH 7.4 ; OC 6%
BHW
pH 7.5 ; OC 7%
WS
pH 7.7 ; OC 3%
SRA
pH 7.8 ; OC 4%
SRW
pH 8.0 ; OC 5%
time (days)

Figure 4

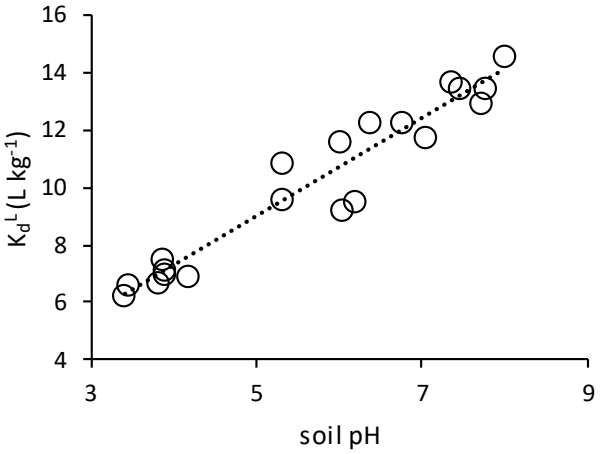

Kinetics of uranium(VI) lability and solubility in aerobic soils

M. Izquierdo[ab]*, S.D. Young[a], E.H. Bailey[a], N.M.J. Crout[a], S. Lofts[c], S.R. Chenery[d] and G. Shaw[a]

[a]School of Biosciences, University of Nottingham, Sutton Bonington Campus, Loughborough, LE12 5RD, United Kingdom
[b]Institute of Environmental Assessment and Water Research, 18-26 Jordi Girona, Barcelona 08034, Spain
[c]UK Centre for Ecology and Hydrology, Lancaster Environment Centre, Library Avenue, Bailrigg, Lancaster, LA1 4AP, United Kingdom
[d]British Geological Survey, Environmental Science Centre, Keyworth, Nottingham, NG12 5GG, United Kingdom

*corresponding author: maria.izquierdo@idaea.csic.es Tel. +34934006146

Supplementary Information

Figure S1. The comparison between observed and modelled U_{sol} (a) and U_E (b) using Eq.5 for the full dataset.

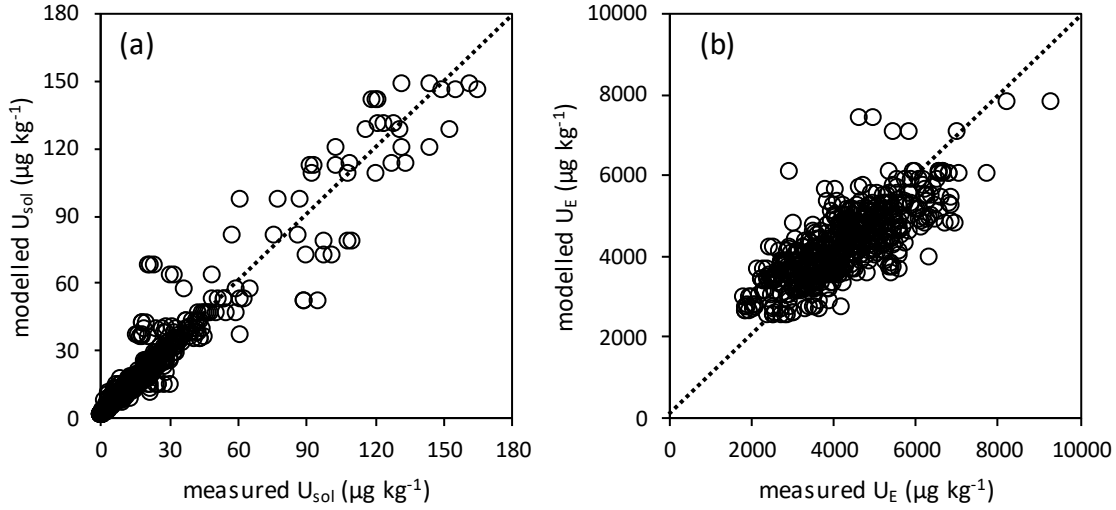

Figure S2. Relationships between soil pH, organic C (OC), free iron oxides Fe_{AM} and modelled kinetic parameters for U_{sol} including A, B and $T_{1/2}$. Several outliers have been identified.

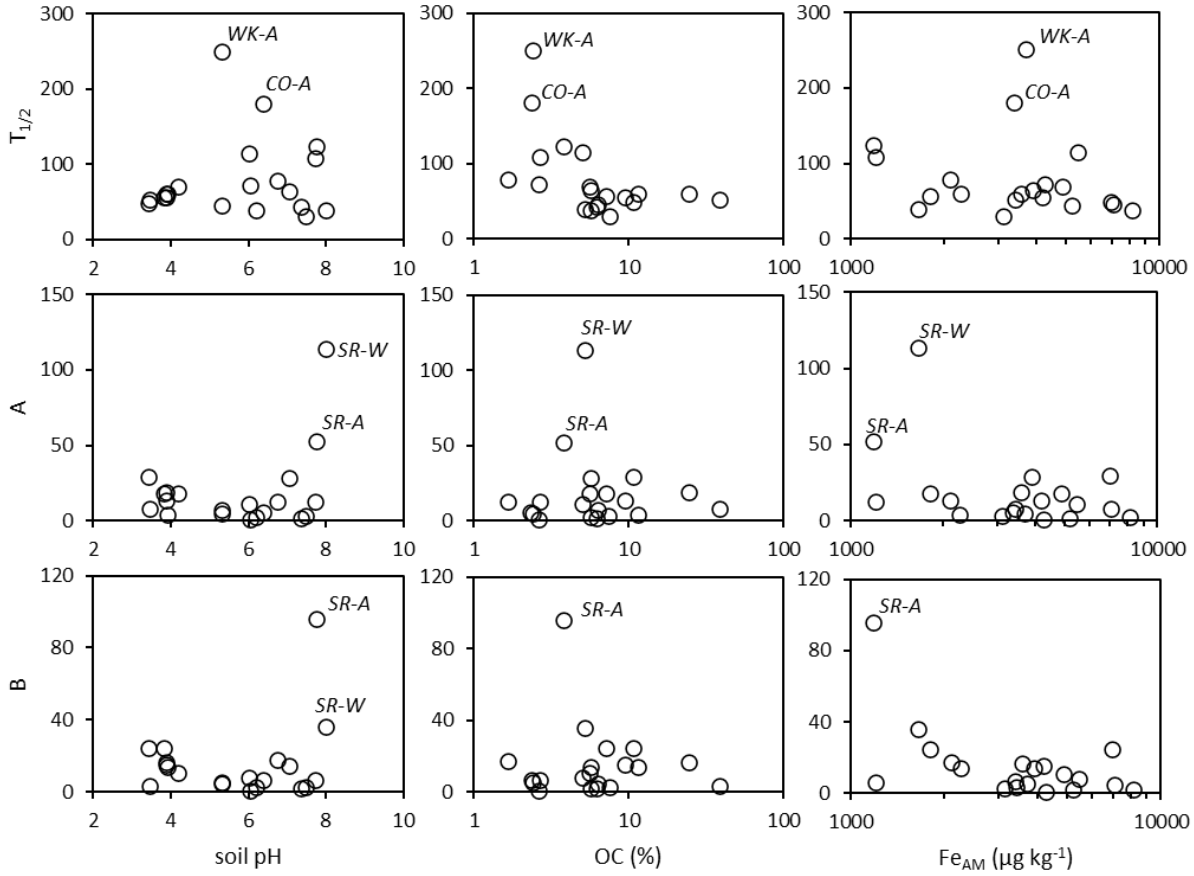

Figure S3. Predicted distribution of aqueous uranyl species across the pH range in two scenarios i.e. preventing and enabling formation of colloidal HFO with surface charge. Model outputs are plotted as defined groups of species including free ion, uranyl complexed with a range of inorganic aqueous ligands and bound to geocolloids (FA, HFO).

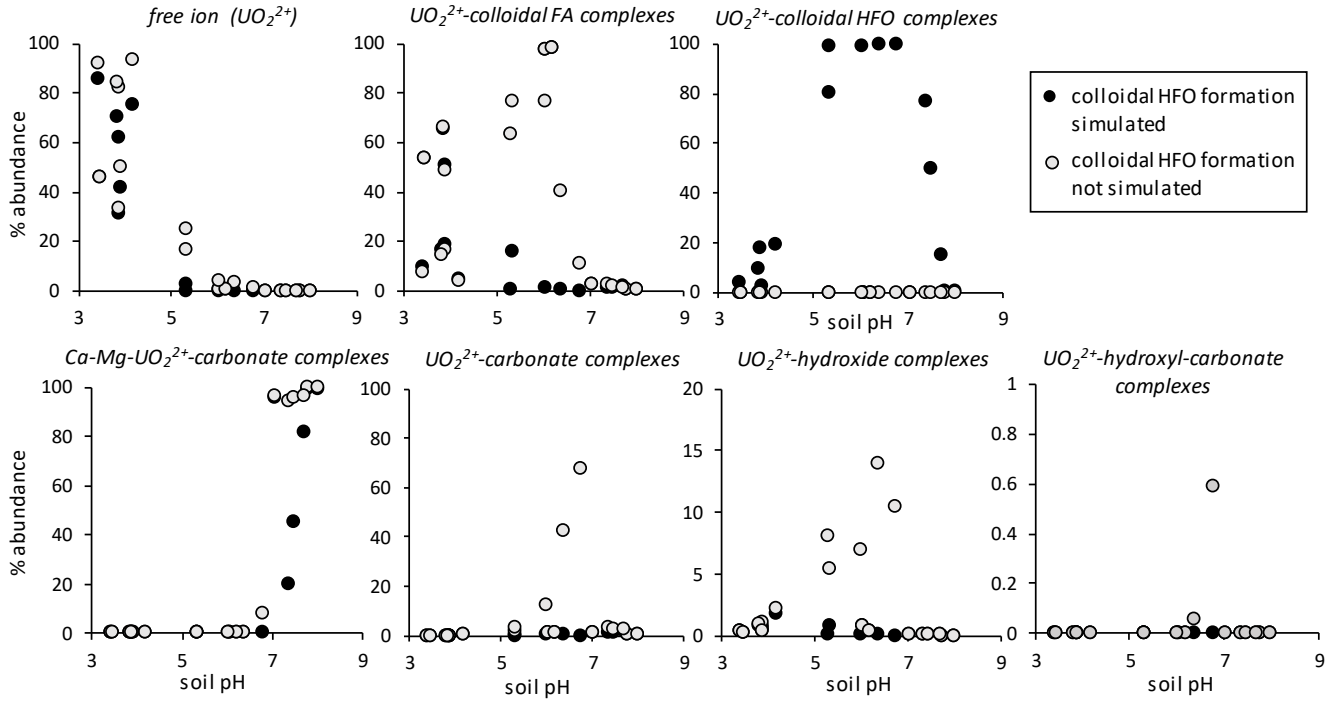

Figure S4. Changes in measured Kd values over the course of the incubation experiment. K_d denotes the partition coefficient between the total U concentration in soil and Usol measured in 0.01M KNO_3 extracts (Eq.3). K_d^L denotes the partition coefficient between the adsorbed and isotopically exchangeable U and the uranyl present as free ion in the 0.01M KNO_3 extracts (Eq. 4).

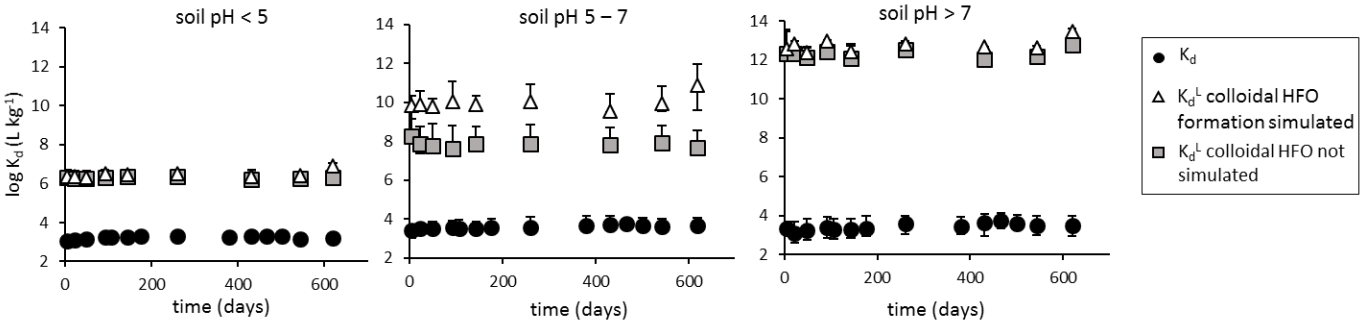

Figure S5. Relationships between U Kd and selected soil properties including (a) soil pH, and two linear relationships for pH 3 – 6 (R^2=0.49) and pH 6 – 8 (R^2=0.28); (b) total organic C content in soil; and (c) concentration of free, amorphous Fe oxides and a linear relationship (R^2=0.30).

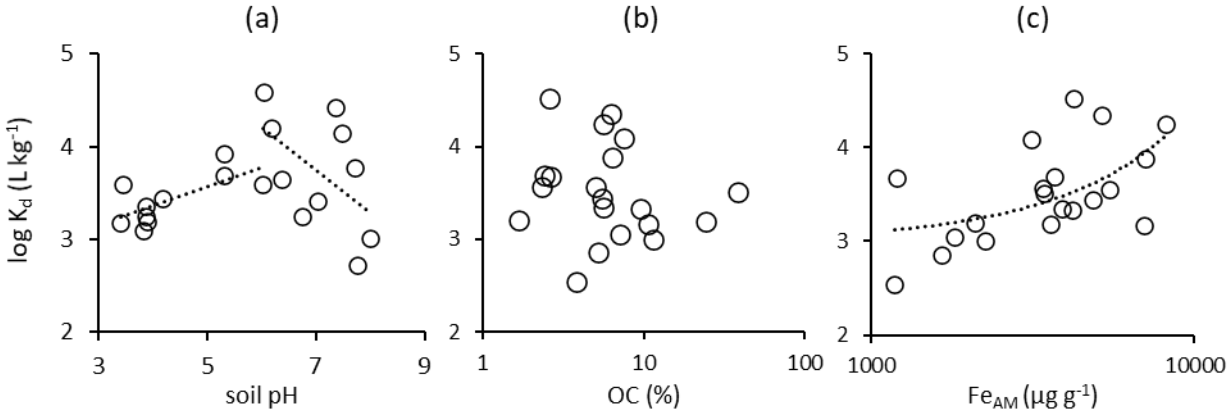

Figure S6. Relationship between soil pH and the chemical exchangeability of U after 4 days incubation. Data split in two subsets i.e. acidic + near neutral (pH < 7; linear relationship R^2=0.53) and calcareous soils (pH > 7, R^2=0.30).

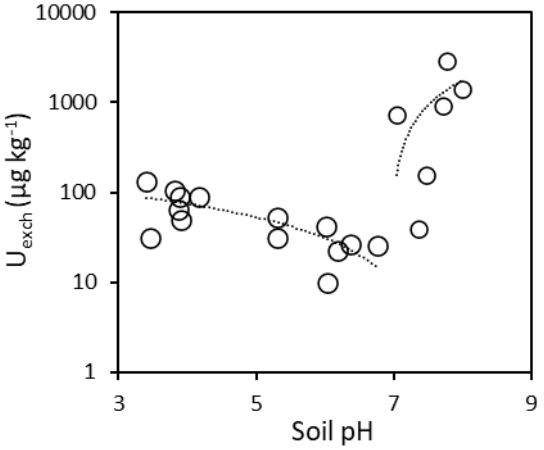

Figure S7. WHAM7 outputs using labile U_E after 619 days incubation as input data: (a) Comparison between observed and predicted U_{sol} concentrations at 619 days. The solid line is the 1:1 line whilst dashed lines represent ±1RSD. (b) Proportion of the solid phases that the labile pool of U_E are associated with. Modelling options includes humic substances and Fe_{AM} and Mn_{AM} as particulate binding phases, and Fe_{sol} and FA as colloidal binding phases. Outliers (i.e. beyond ±1RSD) correspond to low U_{sol}, low Fe_{sol} near neutral EV-A and FD-G soils.

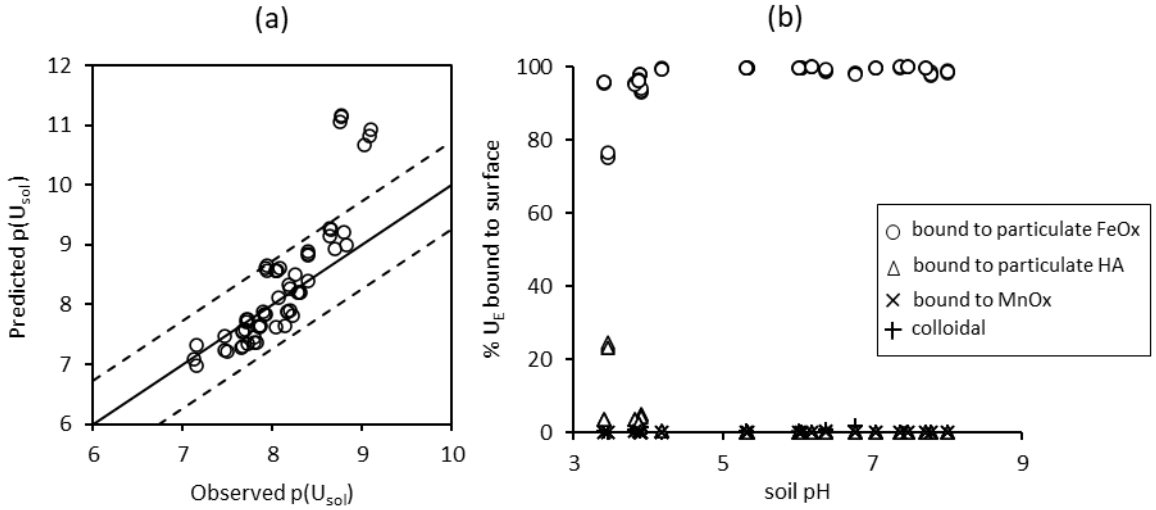

Figure S8. Comparison between observed and predicted concentrations of U_{sol} using WHAM7 when colloidal HFO is not allowed to precipitate in the modelling options. The solid line represents the 1:1 whilst dashed lines represent ±1RSD.

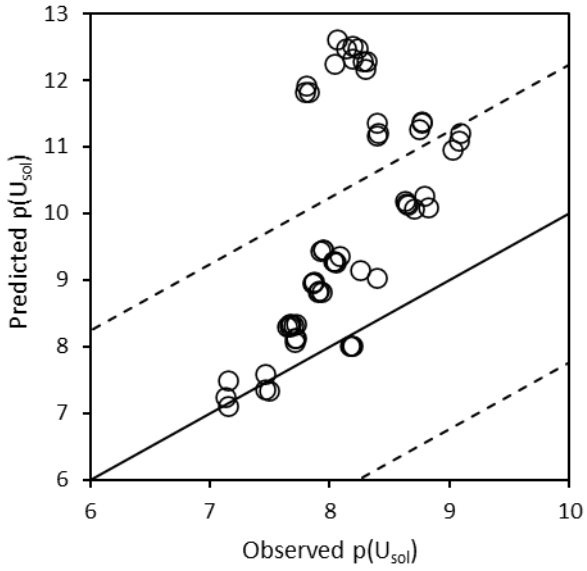

Table S1. Modelled kinetic parameters for U_{sol}.

	T1/2	A	B
	days	µg g^{-1}	µg g^{-1}
BY-W	49	30	25
DY-M	53	8	4
PE-W	57	18	25
WK-W	61	19	17
IH-W	56	14	15
DY-G	61	4	14
BC-M	70	18	11
WK-A	251	5	6
TK-G	46	7.7	4.84
SB-G	115	11	8
EV-A	73	1	1
FD-G	39	3	3
CO-A	181	6	7
NP-A	79	13	18
SR-G	65	29	14
BH-G	44	2	2
BH-W	31	4	3
WS-A	109	13	7
SR-A	124	53	96
SR-W	39	114	36

Table S2. Modelled kinetic parameters for U_E.

	T1/2	A	B
	days	µg g^{-1}	µg g^{-1}

BC-M	201	2194	2893
DY-G	204	2122	3108
DY-M	516	2130	2196
IH-W	66	2359	3811
PE-W	100	2775	3335
WK-W	376	2325	2611
BY-W	80	2399	3548
CO-A	136	2139	3170
EV-A	77	5312	2668
FD-G	24	3673	4103
NP-A	93	3037	2509
SB-G	466	3132	2381
TK-G	74	4223	3357
WK-A	368	1479	3289
BH-G	167	2755	3357
BH-W	348	2514	2298
SR-A	263	3662	1658
SR-G	92	1900	3669
SR-W	245	2231	2912
WS-A	33	3670	1743